THE JOURNAL OF PHYSICAL CHEMISTRY B

 VOLUME 108, NUMBER 23, JUNE 10, 2004

LETTERS

Synthesis of Nickel Hydroxide Nanoribbons with a New Phase: A Solution Chemistry Approach

Dongning Yang,[†] Rongming Wang,[‡] Jin Zhang,*[,†] and Zhongfan Liu*[,†]

Centre for Nanoscale Science and Technology, College of Chemistry and Molecular Engineering, and Electron Microscopy Laboratory and State Key Laboratory for Mesoscopic Physics, School of Physics, Peking University, Beijing 100871, P.R. China

Received: November 25, 2003; In Final Form: February 16, 2004

We report here the successful synthesis of one-dimensional (1D) nanoribbons of nickel hydroxide crystallized in a new phase. This attempt is based on the treatment of freshly precipitated nickel hydroxide with high concentrations of nickel sulfate. The nanoribbons with monoclinic structure had a chemical composition of $Ni(OH)_{1.66}(SO_4)_{0.17}(H_2O)_{0.29}$, which was close to that of α-$Ni(OH)_2$. These nanoribbons were very pure single crystals, structurally uniform with typical widths of 5−25 nm, thicknesses of 1−5 nm, and lengths of up to a few micrometers, and could be an ideal system for studying the physical and chemical properties of 1D nanostructured electrode materials.

One-dimensional (1D) nanostructures, such as nanoscale tubes, wires, rods, and belts (or ribbons), are of great importance from both fundamental and applied perspectives.[1−3] Recently, 1D nanostructured electrode materials have attracted considerable scientific interest due to their potential in boosting the performance of rechargeable batteries.[4−6] In addition, it may be possible, using such materials, to fabricate rechargeable batteries at the nano or micro level.[7] Nickel hydroxide is particularly important in this context since it is an important cathode material in a number of rechargeable battery systems (e.g., Ni/Cd, Ni/H_2, Ni/MH, Ni/Fe, and Ni/Zn).[8] To date, however, it has been extremely difficult to synthesize pure, 1D single nanocrystals of nickel hydroxide for this purpose.[6,9] In this paper we describe the successful synthesis of 1D nanoribbons of nickel hydroxide crystallized in a novel phase.

Our approach is based on the treatment of freshly precipitated nickel hydroxide with high concentrations of nickel sulfate. In a typical experiment, 1.3 g of $Ca(OH)_2$ (0.017 mol) was dispersed in 40 mL of deionized water and added to a solution of 13.0 g of $NiSO_4 \cdot 6H_2O$ (0.049 mol) in 160 mL of deionized water at room temperature. To prevent carbonate incorporation, the deionized water was boiled before use and the experimental process was completed in a nitrogen atmosphere. The pH value of the solution after addition was about 6.5. After the reaction, the concentration of $NiSO_4$ in the mother solution was about 0.16 mol/L. The resulting mixture including freshly precipitated nickel hydroxide was then transferred to a Teflon flask (SLZPI model, 250 mL, from Zhenghong Plastic Factory), sealed, and treated at 100 °C for 24 h. The pH of the solution did not change at the end of the treatment. After the hydrothermal process was complete, the green precipitates were filtered and washed repeatedly with copious amounts of distilled water to remove the byproducts. Since the amount of $CaSO_4$ in the byproducts is 2.3 g and the solubility of $CaSO_4$ in water at room temperature is only 0.002 g/mL, more than 1150 mL of water was needed

* To whom correspondence should be addressed. Phone, Fax: 00-86-10-6275-7157. E-mail: jzhang@chem.pku.edu.cn (J.Z.); lzf@chem.pku.edu.cn (Z.L.).
[†] Center for Nanoscale Science and Technology.
[‡] Electron Microscopy Laboratory and State Key Laboratory for Mesoscopic Physics.

10.1021/jp0375867 CCC: $27.50
Published on Web 05/18/2004

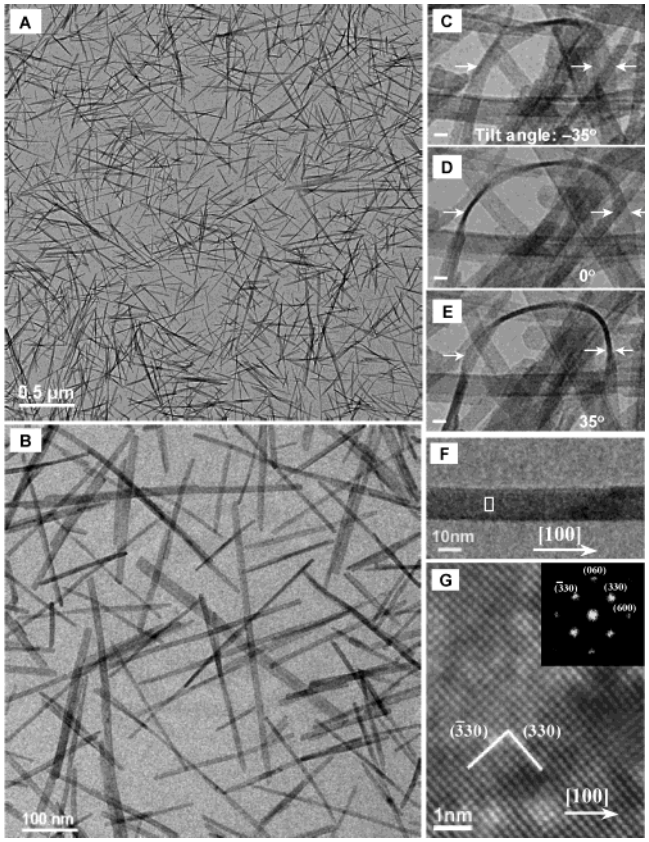

Figure 1. (A, B) TEM images of the products at different magnifications. (C−E) TEM images of the products observed at three different tilt angles. Scale bar: 10 nm. (F) TEM image of a nanoribbon growing along [100]. (G) HRTEM image from a box in F; the inset is the corresponding FFT of the image.

to remove the byproducts. The final products were dried in a vacuum at 50 °C for 24 h.

The nanostructures and morphologies of the products were characterized by transmission electron microscopy (TEM) and high-resolution TEM (HRTEM). Low-magnification TEM images (Figure 1A and B) revealed that the products consisted almost exclusively of a large number of ribbonlike nanostructures. This was deduced from the fact that widths of the nanostructures changed with the tilt angles (−35, 0, and +35°). Parts C−E of Figure 1 show a typical example. The nanoribbons had typical lengths in the hundred nanometer to micrometer range, with thicknesses of 1−5 nm and widths of 5−25 nm. Analysis of a number of nanoribbons with different widths revealed that individual nanoribbons were uniform in width.

Energy-dispersive X-ray (EDX) spectroscopy in scanning TEM (STEM) mode was used to investigate the chemical composition of the nanoribbons. STEM images were collected by a high-angle annular dark field detector (HAADF). A typical image is shown in Figure 2A. Compositional EDX profiles show well-correlated nickel, oxygen, and sulfur signals across the nanoribbons (Figure 2B).

Elemental analysis of the products using X-ray fluorescence (XRF) spectroscopy and thermogravimetric analysis (TGA) provided more quantitative data. This revealed a stoichiometry of $Ni(OH)_{1.66}(SO_4)_{0.17}(H_2O)_{0.29}$ which was close to that of the α-nickel hydroxide reported by Kamath et al.[10] The absence of calcium in the elemental analysis indicated that $CaSO_4$ was completely removed during washing of the products. It has long been known that nickel hydroxide has a hexagonal layered structure with two phases, α and β.[11] The α-phase consists of a hydrotalcite-like structure, having the composition $Ni(OH)_{2-x}(A^{n-})_{x/n}\cdot yH_2O$, where $x = 0.2-0.4$, $y = 0.6-1$, and A = chloride, sulfate, nitrate, carbonate, or other anions.[10,12] The β-phase is isostructural with brucite and does not contain any intercalated anions.

The crystallographic structure of the nanoribbons was examined by X-ray powder diffraction (XRD, performed with Cu Kα radiation on a Rigaku Dmax/2000 diffractometer in the 2θ range of 2 to ∼80°). A typical XRD pattern is given in Figure 3. Neither the positions of the peaks nor their relative intensities corresponded to either of the two known phases, α-$Ni(OH)_2$ or β-$Ni(OH)_2$.[10,13,14]

The strongest six peaks (7.10, 5.126, 3.837, 2.940, 2.232, 1.991 Å) were close to those of paraotwayite (6.81, 5.083, 3.859, 2.946, 2.239, 1.973 Å), a mineral with monoclinic structure and lattice parameters of $a = 7.89$ Å, $b = 2.96$ Å, $c = 13.63$ Å, and $\beta = 91.1°$.[15] However, the first peak (12.6 Å) of the pattern was not reported in the literature and the second peak (8.74 Å) was not close to the corresponding peak of paraotwayite (7.95 Å).[15] While some peak positions were fairly close to paraotwayite, their relative intensities were somewhat different. Moreover, the lattice parameters of paraotwayite or their modifications were not in agreement with the HRTEM results of the nanoribbons.

Another difference between the products and paraotwayite was chemical composition. The empirical formula for

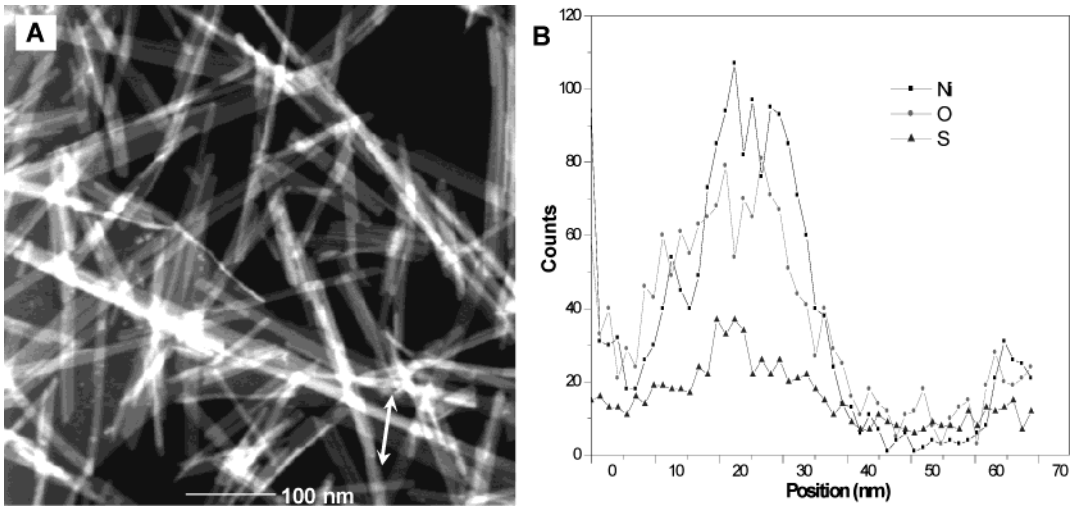

Figure 2. (A) STEM image of the products. (B) The compositional line profiles probed by EDX along the white double-arrow line in 2A.

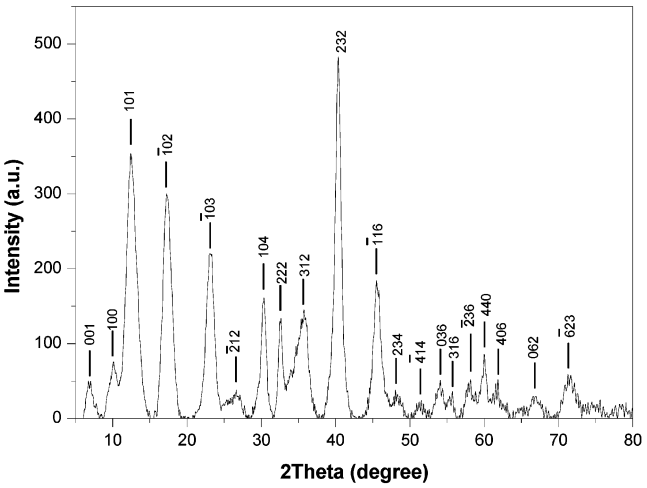

Figure 3. XRD pattern of the products. The numbers above the peaks correspond to the (*hkl*) values of the monoclinic structure.

paraotwayite was $Ni_{0.99}Mg_{0.01}(OH)_{1.43}(SO_4)_{0.17}(CO_3)_{0.12}\cdot 0.37H_2O$, and the generalized anhydrous formula could be written $Ni(OH)_{2-x}(SO_4,CO_3)_{0.5x}$, where x is approximately 0.6.[15] The composition of paraotwayite was close to that of the hydroxy-rich basic salts of nickel, which were isostructural with α-$Ni(OH)_2$ and had the composition $Ni(OH)_{2-x}(A^{n-})_{x/n}\cdot yH_2O$, where $x = 0.5-1$.[12] The nanoribbons had a higher ratio of hydroxyl to metal than paraotwayite.

After detailed analysis it was concluded that this pattern corresponded to a novel phase for nickel hydroxide. The peaks in Figure 3 were indexed as a monoclinic unit cell, and the lattice parameters were calculated to be $a = 8.74(1)$ Å, $b = 8.60(1)$ Å, $c = 12.58(2)$ Å, and $\beta = 91.2(2)°$ with PowderX.[16] In addition, the (222) and (232) peaks were sharper than the (101) peak, indicating anisotropy in the crystallite size.

Figure 1G depicts a lattice-resolved HRTEM image of a nickel hydroxide nanoribbon shown in Figure 1F. This image clearly reveals ($\bar{3}30$) and (330) atomic planes with spacings of 0.201(2) and 0.201(2) nm, respectively. The inset shows the fast Fourier transform (FFT) of the digital HRTEM image. Systemic TEM and HRTEM investigations revealed that the as-synthesized nanoribbons were single crystals with a preferential [100] growth direction along their long axes.

When NaOH was used to replace $Ca(OH)_2$, large numbers of nanoribbons could still be obtained. To confirm the role of $NiSO_4$ in the treatment process, we replaced $NiSO_4$ by $Ni(NO_3)_2$ or $NaSO_4$ with all the other conditions (including pH) remaining the same. Few nanoribbons were observed. When the concentration of nickel sulfate in the treatment process was below 0.008 mol/L and the pH value was kept unchanged, most of the final products were particles. All of the above indicated that high concentrations of nickel sulfate were necessary in the treatment process for the synthesis of the nanoribbons.

We speculate that to produce these nanoribbons during the treatment process, the seeds of nickel hydroxide with monoclinic structure were formed by the chemical interaction between high concentrations of nickel sulfate and freshly precipitated nickel hydroxide. The high concentrations of nickel sulfate as impurities could result in the formation of two-dimensional layers of nickel and sulfate ions on the (010) and (001) faces of the seeds, which might inhibit the growth rate of these two faces.[17−19] Preferential growth in the [100] direction would lead to the growth of the nanoribbon structures described. The formation of novel nickel hydroxide nanoribbons is an example of the crucial role that impurities can play in determining both the morphology and crystallographic structure of crystals grown in solution.

In summary, nanoribbons of nickel hydroxide with monoclinic structure were synthesized by treating freshly precipitated nickel hydroxide with high concentrations of nickel sulfate. These nanoribbons with the chemical composition of $Ni(OH)_{1.66}(SO_4)_{0.17}(H_2O)_{0.29}$ had typical lengths in the hundred nanometer to micrometer range, with thicknesses of 1−5 nm and widths of 5−25 nm. These single-crystalline nanoribbons could be an ideal system for fully studying physical and chemical properties of 1D nanostructured electrode materials.

Acknowledgment. This work was supported by the National Natural Science Foundation of China (NSFC 30000044, 90206023), Ministry of Science and Technology of China (2001CB6105, 2002CB613505), and the FOK YING TUNG Education Foundation (94012). We are grateful for the help from Professor Colin Robinson. We also thank Li Linyan, Liao Fuhui, and Dr. Li Guobao for assistance with the XRD analyses.

References and Notes

(1) Hu, J. T.; Odom, T. W.; Lieber, C. M. *Acc. Chem. Res.* **1999**, *32*, 435.
(2) Xia, Y. N.; Yang, P. D.; Sun, Y. G.; Wu, Y. Y.; Mayers, B.; Gates, B.; Yin, Y. D.; Kim, F.; Yan, H. Q. *Adv. Mater.* **2003**, *15*, 353.
(3) (a) Pan, Z. W.; Dai, Z. R.; Wang, Z. L. *Science* **2001**, *291*, 1947. (b) Shi, W. S.; Peng, H. Y.; Wang, N.; Li, C. P.; Xu, L.; Lee, C. S.; Kalish, R.; Lee, S. T. *J. Am. Chem. Soc.* **2001**, *123*, 11095.
(4) Che, G. L.; Lakshmi, B. B.; Fisher, E. R.; Martin, C. R. *Nature* **1998**, *393*, 346.
(5) Dominko, R.; Arcon, D.; Mrzel, A.; Zorko, A.; Cevc, P.; Venturini, P.; Gaberscek, M.; Remskar, M.; Mihailovic, D. *Adv. Mater.* **2002**, *14*, 1531.
(6) Reisner, D. E.; Salkind, A. J.; Strutt, P. R.; Xiao, T. D. *J. Power Sources* **1997**, *65*, 231.
(7) Dewan, C.; Teeters, D. *J. Power Sources* **2003**, *119*, 310.
(8) Ovshinsky, S. R.; Fetcenko, M. A.; Ross, J. *Science* **1993**, *260*, 176.
(9) Matsui, K.; Kyotani, T.; Tomita, A. *Adv. Mater.* **2002**, *14*, 1216.
(10) Kamath, P. V.; Therese, G. H. A.; Gopalakrishnan, J. *J. Solid State Chem.* **1997**, *128*, 38.
(11) (a) Oliva, P.; Leonardi, J.; Laurent, J. F.; Delmas, C.; Braconnier, J. J.; Figlarz, M.; Fievet, F. *J. Power Sources* **1982**, *8*, 229. (b) Oswald, H. R.; Asper, R. In *Preparation and Crystal Growth of Materials with Layered Structure*; Lieth, R. M. A., Ed.; D. Reidel: Dordrecht, The Netherlands, 1977.
(12) Rajamathi, M.; Kamath, P. V. *J. Power Sources* **1998**, *70*, 118.
(13) Rajamathi, M.; Kamath, P. V.; Seshadri, R. *J. Mater. Chem.* **2000**, *10*, 503.
(14) *Joint Committee on Powder Diffraction Standards (JCPDS)*, file No. 14-117; International Center for Diffraction Data: Swathmore, PA.
(15) Nickel, E. H.; Graham, J. *Can. Mineral.* **1987**, *25*, 409.
(16) Dong, C. *J. Appl. Crystallogr.* **1999**, *32*, 838.
(17) Verdaguer, S. V. *Prog. Cryst. Growth Charact.* **1996**, *32*, 75.
(18) Sangwal, K. *Prog. Cryst. Growth Charact.* **1996**, *32*, 3.
(19) Sangwal, K. *J. Cryst. Growth* **1999**, *203*, 197.